geoconvention
Calgary • Canada • June 20-22 2022

Tectonic structure and Cenozoic Structural Evolution of the Enping Sag, Pearl River Mouth Basin, northern South China Sea margin

Jie Zhang[1,2], Zhiping Wu[1], Elena Konstantinovskaya[2], Yanjun Cheng[1]
[1]School of Geosciences, China University of Petroleum (East China),
[2]Earth and Atmospheric Sciences, University of Alberta

Summary

The Pearl River Mouth Basin is located at the continental shelf and slope of northern South China Sea. The petroleum plays of the basin are largely controlled by tectonic structure and Cenozoic evolution of the region. A series of syn-rift normal fault systems that bound numerous Tertiary sags and uplifts of the basin formed during the Eocene - Early Oligocene extension of the South China margin. The emplacement of normal faults and syn- and post-rift subsidence contributed to accumulation of deltaic sand-rich and carbonate platform deposits, source rock maturation, hydrocarbon migration and emplacement of structural traps. The Enping Sag represents one of the Tertiary sags located on the continental shelf at the depth interval of the oil generation window. This paper aims to analyze systems of normal faults and Cenozoic tectonic evolution of the Enping Sag based on the interpretation of high-density 2-D and 3-D seismic surveys and well data. A better understanding of fault architecture and fault transmissibility in the Enping Sag will contribute to the hydrocarbon exploration of the study area.

Geologic background

The Enping Sag is located in the west Zhu I Sub-Basin of the Pearl River Mouth Basin (Fig. 1a) that represents a NE-SW elongated rift zone (Ye et al., 2018).

The Cenozoic sedimentary succession of the Pearl River Mouth Basin includes syn-rift deposits of the Eocene Wenchang (E_2w) and Lower Oligocene Enping (E_2e) Formations; post-rift deposits of the Upper Oligocene Zhuhai (E_3z), Lower Miocene Zhujiang (N_1z), Middle Miocene Hanjiang (N_1h), Upper Miocene Yuehai (N_1y) and Pliocene Wanshan (N_2w) Formations and Quaternary (Q) strata (Liu et al., 2016). The source rocks consist of Wenchang lacustrine mudstones and coal measures of the Enping Formation that are mature in the Enping 17 Sub-Sag (Fig. 1a) (Zhang et al., 2015). The reservoir rocks are present both in syn-rift and post-rift formations. Most of the oil discoveries are located in the Oligocene Zhuhai deltaic deposits and Lower Miocene Zhujiang sand-rich deltaic to carbonate platform deposits (Zhang et al., 2015; Peng et al., 2016; Liu et al., 2016). The main unconformities are recognized at the base of syn-rift and post-rift units. The sealing units consist mudstones mostly present in the post-rift Miocene deposits.

The Enping Sag is limited by the Northern Uplift in the north and by the Panyu Lower Uplift in the south (Fig. 1a). The Enping Sag consists of the 17 and 12 Sub-Sags bounded by the NE-SW EP17 Fault in the northwest, and the 18 Sub-Sag bounded in the north by the EP18 Fault (Fig. 1a). The structural traps in the Enping Sag are associated with tilted fault blocks and rollover anticlines (Liu et al., 2011).

The total geological reserves of the Enping Sag are estimated 8.43*10^8 m^3 (5.3*10^9 bbl) of oil equivalent (Xiong et al., 2020).

Methods

This study is based on integrated analysis of 2D and 3D offshore seismic reflection data and well data provided by the China National Offshore Oil Corporation (CNOOC). The structural seismic interpretation, analysis of fault geometry and transmissibility and isopach maps were performed in Geoframe and Petrel.

Results

The syn-rift faults of the Enping Sag are oriented NE-SW and near E-W (Fig.1b). The main boundary fault that delineates the 17 and 12 Sub-Sags in the northwest is the SE-dipping listric low-angle normal EP17 Fault with vertical throw of up to 1 s TWT. The fault is curved in map view, it extends for about 60 km along the strike, and it flattens into a sub-horizontal detachment at about 4.8 s TWT (Fig. 1c-d).

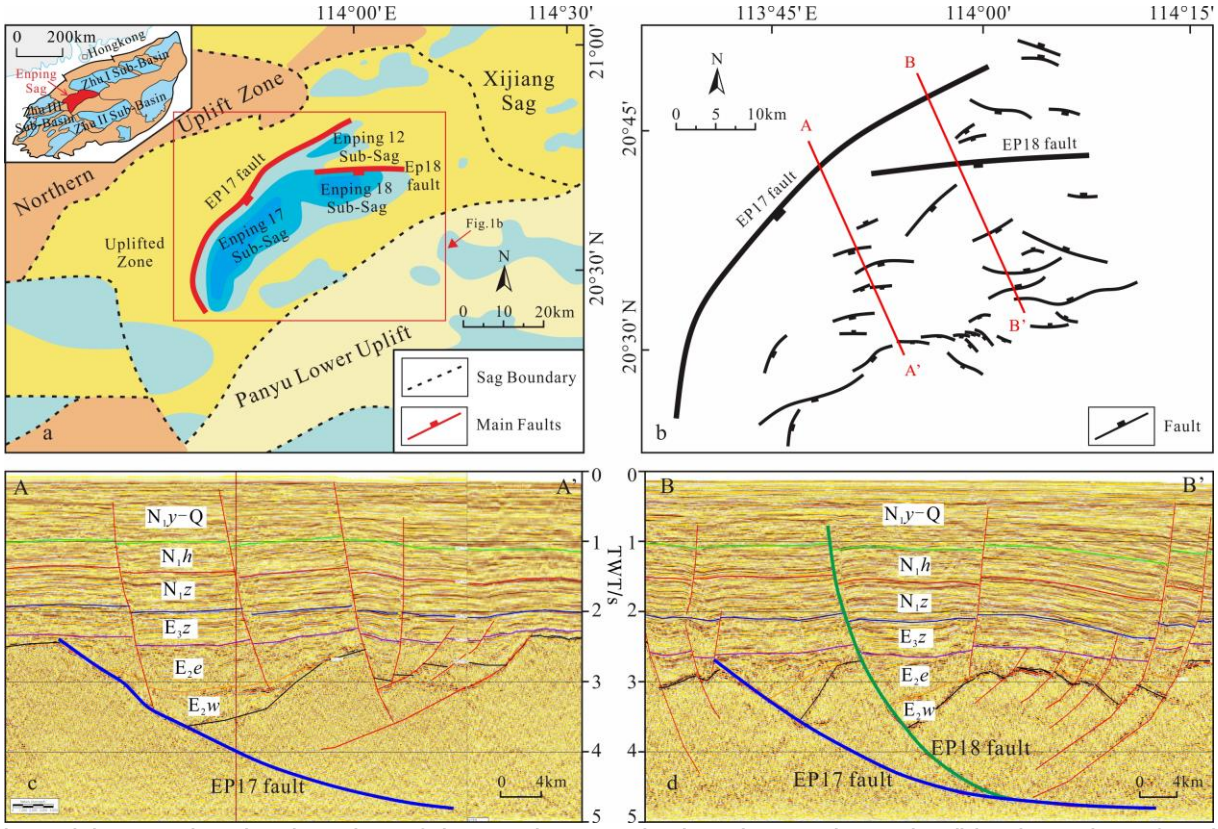

Fig. 1 (a) Map showing location of the Enping Sag in the Zhu I Sub-Basin; (b) orientation of main Cenozoic faults in the Enping Sag; (c) and (d) interpreted NW-SE seismic lines across the 17 Sub-Sag (A-A') and 18, 12 Sub-Sags (B-B') of the Enping Sag.

The E-W boundary fault EP18 dips to the south and it defines the EP18 Sub-Sag in the north extending along the strike for about 25 km (Fig. 1a). The EP18 Fault is a growth fault with dip and amount of vertical displacement varying with depth (Fig. 1d). The fault flattens and merges into the EP17 Fault at the depth, and it is steep in the upper portion extending up to Miocene post-rift deposits. The vertical displacement along the EP18 Fault ranges from about 1 s TWT in the syn-rift units to about 10-50 ms TWT in the post-rift Miocene units. The synthetic and antithetic conjugated listric faults delineate the syn-rift sub-basins of 17, 12 and 18 Sub-Sags with vertical throw up to about 500 ms TWT. Most of the syn-rift faults cannot be traced above the top of the Lower Oligocene Enping (E_2e) Formation (Fig.1c-d). A series of the WNW-ESE and E-W high-angle trans-tensional right-lateral strike-slip faults displace the Miocene post-rift deposits. The vertical offset along the reactivated post-rift faults is about 10-50 ms.

The NE-SW and ENE-WSW syn-rift listric normal faults were emplaced during the Early to Middle Eocene (E_2w). The Enping Sag was formed as a detached half graben controlled by the SE-dipping low angle normal detachment EP17 Fault. The E-W syn-rift growth normal faults were emplaced in the Late Eocene to Early Oligocene (E_2e), and accommodated the eastward and southward migration of the depocenters. During this time, the displacement along the EP17 fault gradually decreased along the strike from the southwest to the northeast, and most of the extension was accommodated by the syn-rift E-W EP18 fault and conjugated faults. The WNW-ESE and E-W trans-tensional right-lateral strike-slip faults developed during the tectonic reactivation phase that started in the Late Miocene. These faults controlled subsidence and sedimentation in upper post-rift succession.

The tectonic phases recognized in the Enping Sag can be correlated with Cenozoic evolution of the northern South China Sea continental margin. The retreat of subduction zone of the Pacific Plate during the Early to Middle Eocene (E_2w) resulted in the NW-SE extension in the overlying plate of the South China Sea margin (Hall, 2002), and the emplacement of the NE-SW and ENE-WSW syn-rift normal faults in the Enping Sag. The rotation of Pacific Plate motion from NNW to WNW and the India-Eurasian collision during the Late Eocene to Early Oligocene (E_2e) resulted in the clockwise rotation of extension from NW-SE to N-S in the study area, and the emplacement of the E-W syn-rift fault system of the Enping Sag (Tapponnier et al., 1986; Meng et al., 2012). Post-rift subsidence, sedimentation and fault reactivation occurred in the Enping Sag during the intra-continental rifting and seafloor spreading on the South China continental margin in the Late Oligocene to Middle Miocene (Wu and Suppe, 2018). The Late Miocene tectonic plate reconstruction resulted in the NE-SW shortening and reactivation of the pre-existing WNW-ESE and E-W normal faults as trans-tensional right-lateral strike-slip faults in the Enping Sag.

Acknowledgments

We thank CNOOC Ltd for providing 2D and 3D seismic data and well data used in this study; Schlumberger for the consolidated license donation to the University of Alberta. This work is funded by China National Science and Technology Major Project (2016ZX05024-002-001), the China Scholarship Council (202106450035) and NSERC through grants RGPIN 2019 04397 and DGECR 2019 00186.

References

Hall, R., 2002. Cainozoic Geological and Plate Tectonic Evolution of SE Asia and the SW Pacific: Computer-Based Reconstructions, Model and Animations. Journal of Asian Earth Sciences, 20(4): 353-431. https://doi.org/10.1016/S1367-9120(01)00069-4

Liu, L.H., Chen, S.H., Yu, S.M., Xiong, J.Y., Jiang, J., Xu, X.M., Liu, X.L., Hu, K., 2011. Analyzing conditions of hydrocarbon accumulation and a commercial breakthrough in Enping sag, Pearl River Mouth basin. China Offshore Oil and Gas, 23(2): 76-80. doi: 10.3969/j.issn.1673-1506.2011.02.002

Liu, Q.H., Zhu, H.T., Shu, Y., Zhu, X.M., Yang, X.H., Chen, L., Tan, M.X., Geng, M.Y., 2016. Provenance identification and sedimentary analysis of the beach and bar systems in the Palaeogene of the Enping Sag, Pearl River Mouth Basin, South China Sea. Marine and Petroleum Geology, 70: 251-272. http://dx.doi.org/10.1016/j.marpetgeo.2015.12.002

Meng, J., Wang, C.S., Zhao, X.X., Coe, R., Li, Y.L., Finn, D., 2012. India-Asia Collision was at 24°N and 50 Ma: Palaeomagnetic Proof from Southernmost Asia. Scientific Reports, 2(1): 1-11. https://doi.org/10.1038/srep00925.

Peng, J.W., Pang, X.Q., Shi, H.S., Peng, H.J., Xiao, S., Yu, Q.H., Wu, L.Y., 2016. Hydrocarbon generation and expulsion characteristics of Eocene source rocks in the Huilu area, northern Pearl River Mouth basin, South China Sea: Implications for tight oil potential. Marine and Petroleum Geology 72: 463-487. http://dx.doi.org/10.1016/j.marpetgeo.2016.02.006

Tapponnier, P., Peltzer, G., Armijo, R., 1986. On the Mechanics of the Collision between India and Asia. Geological Society, London, Special Publications, 19(1): 113-157. https://doi.org/10.1144/GSL.SP.1986.019.01.07

Wu, J., Suppe, J., 2018. Proto-South China Sea Plate Tectonics Using Subducted Slab Constraints from Tomography. Journal of Earth Science, 29(6): 1304-1318. https://doi.org/10.1007/s12583-017-0813-x

Xiong, W.L., Zhu, J.Z., Yang, X.Y., Long, Z.L., Zhai, P.Q., Zheng, Y.D., Qin, C.G., 2020. Study on the genetic sources and accumulation processes of oil and gas in the north uplift structural belt of Enping sag. China Offshore Oil and Gas, 32(1): 54-65. doi: 10.11935/j.issn.1673-1506.2020.01.006

Ye, Q., Mei, L.F., Shi, H.S., Shu, Y., Camanni, G., Wu, J., 2018. A low-angle normal fault and basement structures within the Enping Sag, Pearl River Mouth Basin: Insights into late Mesozoic to early Cenozoic tectonic evolution of the South China Sea area. Tectonophysics, 731: 1-16. https://doi.org/10.1016/j.tecto.2018.03.003

Zhang, G.C., Li, J., Lei, L., Zhao, Z., 2015. Analysis of the orderly distribution of oil and gas fields in China based on the theory of co-control of source and heat. Natural Gas Industry B, 1-28. http://dx.doi.org/10.1016/j.ngib.2015.02.005